A FOURIER METHOD FOR THE ANALYSIS OF EXPONENTIAL DECAY CURVES

S. W. PROVENCHER

From the Max-Planck-Institut für biophysikalische Chemie, D-3400 Göttingen-Nikolausberg, Federal Republic of Germany

ABSTRACT A method based on the Fourier convolution theorem is developed for the analysis of data composed of random noise, plus an unknown constant "base line," plus a sum of (or an integral over a continuous spectrum of) exponential decay functions. The Fourier method's usual serious practical limitation of needing high accuracy data over a very wide time range is eliminated by the introduction of convergence parameters and a Gaussian taper window. A computer program is described for the analysis of discrete spectra, where the data involves only a sum of exponentials. The program is completely automatic in that the only necessary inputs are the raw data (not necessarily in equal intervals of time); no potentially biased initial guesses concerning either the number or the values of the components are needed. The outputs include the number of components, the amplitudes and time constants together with their estimated errors, and a spectral plot of the solution. The limiting resolving power of the method is studied by analyzing a wide range of simulated two-, three-, and four-component data. The results seem to indicate that the method is applicable over a considerably wider range of conditions than nonlinear least squares or the method of moments.

INTRODUCTION

There is a wide variety of experiments in which the data are represented by an integral over an exponential (Laplace) kernel:

$$y(t) = \int_0^\infty e^{-\lambda t} s(\lambda)\, d\lambda, \tag{1}$$

and it is desired to determine the "spectrum" $s(\lambda)$ from a set of n experimentally measured values of $y(t)$ of limited accuracy. Such problems arise in the relaxation kinetics of cooperative conformational changes in biopolymers (1, 2) and in sedimentation equilibrium (3–5) and light scattering (6) in polymer solutions. Similar integral equations of the first kind or deconvolution problems occur in areas ranging from instrument broadening in diffraction (7, 8), spectroscopy (9), and chromatography (10) and overlapping excitation in fluorescence decay (11) to aerial broadening (12) in radio astronomy.

The most common form of this problem in biophysics involves "discrete spectra," where the integral in Eq. 1 becomes a sum:

$$y(t) = \sum_{j=0}^{N_\lambda} \alpha_j \exp(-\lambda_j t), \tag{2}$$

and N_λ is usually only of the order of 5 or less. In this case the spectrum may be represented by a sum of Dirac delta functions:

$$s(\lambda) = \sum_{j=0}^{N_\lambda} \alpha_j \delta(\lambda - \lambda_j). \tag{3}$$

We include the possibility of having an unknown instrument "base-line" component α_0 with $\lambda_0 = 0$. Data of this type occur in relaxation (13, 1) and tracer (14) kinetics, fluorescence (11) and radioactive (15) decay, radioisotope exchange kinetics (16), and sedimentation equilibrium in paucidisperse solutions (17).

This problem is especially difficult in biophysics because one is often attempting to determine an unknown mechanism or appropriate model. The presently available methods like (nonlinear) least squares (16, 18–20) or the method of moments (11, 17), require a potentially biased initial guess at N_λ as well as (in the case of least squares) the set of $2N_\lambda + 1$ parameters, $\{\alpha_j, \lambda_j\}$. If the guess is not good enough, the methods can converge to completely incorrect $\{\alpha_j, \lambda_j\}$. Furthermore, because of the well known severe nonorthognality of exponentials, these incorrect $\{\alpha_j, \lambda_j\}$ can still reproduce the data well enough to be accepted, especially if N_λ is unknown (21, 11, 16).

In this paper we develop a method based on an exact formal solution of Eq. 1 by Fourier transforms (22). Although this approach had been used on deconvolution problems (7, 12) similar to Eq. 1, it was Gardner et al. (15, 23) who first used it on discrete spectra. In principle, this method is very attractive since the solution is of the form of a spectrum vs. $\ln \lambda$, with sharp peaks at $\ln \lambda_j$ and with amplitudes proportional to α_j/λ_j. Thus N_λ, as well as $\{\alpha_j, \lambda_j\}$, is automatically determined without any initial assumptions. In practice, their method often gave rather disappointing results with large "error ripples" obscuring the spectrum unless the t range was extremely wide (typically five decades) and the data very accurate. Because of this only a few workers (14, 24) have used this method.

For the analysis of sedimentation equilibrium data Provencher and Gobush (5) modified the Fourier solution of Eq. 1 to include two parameters which make the solution a usable one in spite of a severely restricted t range. In this paper we use these parameters, which will be called β and ϵ, and some additional improvements to develop a method for data of limited accuracy as well as restricted t range. Although the method is applicable to Eq. 1 as well as many similar data deconvolution problems (5–7, 9–12), we defer this for later treatment, and here we specialize to discrete spectra.

In the final section a completely automatic computer program is used to analyze some simulated two-, three-, and four-component data containing pseudorandom errors. The only necessary input to the program are the $y(t)$ and t values (not necessarily in equal intervals of t); no potentially biased information is needed. The

output includes N_λ, $\{\alpha_j, \lambda_j\}$ with their estimated errors, and plots of the spectrum. The effect of such conditions as error level and type, α ratios, λ ratios, knowledge that $\alpha_0 = 0$, t range, n, and N_λ on the limiting resolving power of the method are studied. The results seem to indicate that this method is applicable over a considerably wider range of conditions than the method of moments or least squares.

Over 300 analyses of a wide variety of real and simulated data have been performed without any modifications to the program. Therefore, since a user-oriented FORTRAN IV version together with a detailed description will be available on request, no attempt will be made here to give all the programming details.

FORMAL SOLUTION

We want to solve the following equation for $S(\lambda)$:

$$Y(T) = \int_0^\infty e^{-\lambda T} S(\lambda)\, d\lambda. \tag{4}$$

(The reason for changing the notation of Eq. 1 will be obvious in the next section.) The lower limit is zero simply because it is usually assumed that there is only exponential *decay*, i.e., $S(\lambda) = 0$ for $\lambda < 0$. Thus for arbitrary $\beta > 0$, we can extend the lower limit to $-\beta$. Then, making the changes of variables $T = e^x$ and

$$\lambda = e^{-z} - \beta, \tag{5}$$

and multiplying both sides by $\exp[(1 + \epsilon)x - \beta e^x]$ with $\epsilon > -1$, we can put Eq. 4 in the form of a convolution:

$$g_Y(x) = \int_{-\infty}^\infty g_S(z) g_K(x - z)\, dz, \tag{6}$$

where

$$g_Y(x) = \exp[(1 + \epsilon)x - \beta e^x] Y(e^x), \tag{7}$$

$$g_S(z) = e^{\epsilon z} S(e^{-z} - \beta) = e^{\epsilon z} S(\lambda), \tag{8}$$

$$g_K(x - z) = \exp[-\exp(x - z) + (1 + \epsilon)(x - z)]. \tag{9}$$

If we use $\tilde{g}$ to represent the Fourier transform of g:

$$\tilde{g}(\mu) = \int_{-\infty}^\infty g(x) e^{i\mu x}\, dx, \tag{10}$$

then, by the Fourier convolution theorem (22), the Fourier transform of Eq. 6 is simply $\tilde{g}_Y(\mu) = \tilde{g}_S(\mu)\tilde{g}_K(\mu)$. Solving this for $\tilde{g}_S(\mu)$ and taking an inverse Fourier transform, we get the formal solution:

$$g_S(z) = \frac{1}{2\pi} \int_{-\infty}^\infty \tilde{g}_S(\mu) e^{-i\mu z}\, d\mu, \tag{11}$$

where

$$\tilde{g}_S(\mu) = \tilde{g}_Y(\mu)/\tilde{g}_K(\mu). \tag{12}$$

The Fourier transform of the kernel function, Eq. 9, is a complex gamma function:

$$\tilde{g}_K(\mu) = \Gamma(1 + \epsilon + i\mu), \tag{13}$$

and is evaluated using standard formulas (25). However, $\tilde{g}_Y(\mu)$ must be evaluated numerically from the data:

$$\tilde{g}_Y(\mu) = \int_{-\infty}^{\infty} \exp[(1 + \epsilon)x - \beta e^x + i\mu x]\, Y(e^x)\, dx. \tag{14}$$

Hence the solution involves two main steps: numerical evaluation of the Fourier transform in Eq. 14 and then numerical evaluation of the inverse transform in Eq. 11. We then have our spectrum $S(\lambda)$ by the simple relation in Eq. 8. Our solution reduces to that of Gardner et al. (15) when $\beta = \epsilon = 0$.

METHOD

Autocorrelation Data Smoothing

If the data are in equal intervals, Δt, of t, we use the following smoothing process:

$$Y(T_k) = \sum_{m=1}^{M} y(t_m)y(t_m + T_k) \Big/ \sum_{m=1}^{M} y^2(t_m), \tag{15}$$

where

$$T_k = (k - 1)\Delta t, \qquad k = 1, 2, \cdots N, \qquad N = n - M + 1.$$

We use the conventions that $\{t_m\}$ is in increasing order and that y or Y with a subscripted argument t_k or T_k represents a data point rather than an exact functional value. Like a true autocorrelation function, where $M \to \infty$, this process should tend to reduce uncorrelated noise in the data.

This process is similar to Dyson and Isenberg's "mean displaced ratio" (17), and they have pointed out that for both processes the smoothed data conveniently retains the same $\{\lambda_j\}$ as the raw data without any bias coming in. Substituting Eq. 2 into Eq. 15, one can easily verify that

$$Y(T) = \sum_{j=0}^{N_\lambda} A_j \exp(-\lambda_j T), \tag{16}$$

with

$$A_j = \alpha_j \sum_{m=1}^{M} y(t_m) \exp(-\lambda_j t_m) \Big/ \sum_{m=1}^{M} y^2(t_m). \tag{17}$$

Thus we actually analyze the smoothed $Y(T_k)$ for the spectrum

$$S(\lambda) = \sum_{j=0}^{N_\lambda} A_j \delta(\lambda - \lambda_j) \tag{18}$$

and then convert the $\{A_j\}$ back to $\{\alpha_j\}$ using Eq. 17.

If the data are in equal intervals of t, the program sets $M = n/20$ with the constraint $3 \leq M \leq 5$. Better smoothing could be attained with larger M, but that would further reduce both the T range and the A_j of any components with large λ_j (see Eq. 17). If the data are in unequal intervals of t, the program simply sets $M = 1$ and $T_k = t_k - t_1$. In both cases $Y(T_1) = 1$ and more importantly $T_1 = 0$.

Convergence Parameter β

The most serious limitation of the method of Gardner et al. is that the data must cover a very wide t range. Otherwise, there can be serious cutoff errors in the evaluation of Eq. 14 along their $x = \ln t$ axis with $\beta = \epsilon = 0$. We can easily eliminate the problem at the low t end of the axis by a change of variable in Eq. 14 from x to T:

$$\tilde{g}_Y(\mu) = \int_0^{T_N} \{T^\epsilon e^{-\beta T} Y(T) T^{i\mu}\} \mathrm{d}\, T + \int_{T_N}^{\infty} \{\cdots\} \mathrm{d}T. \tag{19}$$

Since $T_1 = 0$, the only cutoff error is in neglecting the second integral, and this is made small by adjusting β so that the average absolute contribution of the last few data points to $\tilde{g}_Y(0)$ is between 0.02% and 0.04% of the total $\tilde{g}_Y(0)$.

According to Eq. 5, the distance between two spectral peaks corresponding to components with λ_j and λ_k is $|z_j - z_k| = |\ln[(\lambda_k + \beta)/(\lambda_j + \beta)]|$. Thus too large a β reduces the distance between the peaks and hence the resolving power of the method. Thus the program takes the $\{\alpha_j, \lambda_j\}$ obtained using the original β, substitutes it into Eqs. 17 and 16 and then into the second integral in Eq. 19. This integral is then evaluated analytically as a sum of incomplete gamma functions using standard formulas (26). The analysis is then repeated using this improved $\tilde{g}_Y(\mu)$ and a smaller β. The program iterates in this way up to three times, reducing β in three equal steps down to $\beta = \beta_{\min} = 0.2/t_n$, a value small enough not to cause any resolution problems. If the t range is wide enough so that the original $\beta \leq \beta_{\min}$, the program sets $\beta = \beta_{\min}$ and does only one iteration.

The factor $T^{\epsilon + i\mu}$ in Eq. (19) has a singularity at $T = 0$ when $\epsilon < 0$ and oscillates rapidly as $T \to 0$ when $\mu \neq 0$. Thus a special quadrature technique is used that passes parabolas through the well behaved part of the integrand, $e^{-\beta T} Y(T)$, (analogous to Simpson's rule) but accounts exactly for the poorly behaved part $T^{\epsilon + i\mu}$.

Gaussian Taper Window Parameter σ

A second cutoff problem arises in the evaluation of Eq. 11. Substituting Eq. 18 into Eq. 8 and taking its Fourier transform along the z axis, we get the theoretical form of the integrand in Eq. 11:

$$\tilde{g}_S(\mu) = \sum_{j=0}^{N_\lambda} A_j (\lambda_j + \beta)^{-(1+\epsilon)} \exp(i\mu z_j), \tag{20}$$

where

$$z_j = -\ln(\lambda_j + \beta). \tag{21}$$

Thus, even in the absence of errors, $\tilde{g}_S(\mu)$ is a sum of periodic imaginary exponentials, and the integral in Eq. 11 does not converge. However, we can substitute Eq. 20 into Eq. 11, evaluate the integral with the limits $\pm\mu_0$, and take the limit as $\mu_0 \to \infty$:

$$g_S(z) = \sum_{j=0}^{N_\lambda} A_j(\lambda_j + \beta)^{-(1+\epsilon)} \lim_{\mu_0 \to \infty} \left[\frac{\sin\{\mu_0(z_j - z)\}}{\pi(z_j - z)}\right]. \tag{22}$$

The limit of the sinc function in square brackets is a definition of $\delta(z_j - z)$. Thus, in principle, we can get arbitrarily good resolution in the spectrum by performing the integration in Eq. 11 out to large enough μ_0. In practice, as $|\mu|$ increases in Eq. 12, both the analytic function $\tilde{g}_K(\mu)$ and the exact part of $\tilde{g}_Y(\mu)$ rapidly approach zero; however, the high frequency noise components in $\tilde{g}_Y(\mu)$ do not. Thus, for large enough μ, $\tilde{g}_S(\mu)$ rapidly diverges, becoming nearly pure noise amplified disastrously by the very small $\tilde{g}_K(\mu)$ in the denominator of Eq. 12. This is simply a manifestation of the extreme instability of solutions of integral equations like Eqs. 1 or 2, with smooth broad kernels, to errors in the data. Thus any method that attempted to obtain a general solution with all high frequency (i.e., high μ) fine structure would have similar problems.

Thus Gardner et al. cut off the integral in Eq. 11 at $\pm\mu_0$, where the appropriate μ_0 depends on the accuracy and smoothness of the data. Therefore their spectra are of the form of Eq. 22 with $\beta = \epsilon = 0$ and with no limit taken. The sinc function in square brackets in Eq. 22 has the well known form of a peak at $z = z_j$ with an infinite number of extra side peaks decreasing in amplitude only as $1/|z - z_j|$. This form can be seen in the spectra of Gardner et al. (15, 23) and is the main source of the error ripples that tend to obscure the true peaks.

Similar cutoff problems occur in the Fourier inversion of diffraction data (8) and the spectral analysis of random processes (27), where one must estimate an infinite Fourier transform from a finite range of data. It is now well known (8, 27, 28) that by multiplying $\tilde{g}_S(\mu)$ by a more smoothly tapering "window" function (instead of the infinitely sharp "boxcar function" that represents the cutoff used by Gardner et al.) the spectrum will have smaller side peaks at the expense of only slightly broader true peaks. Of the several windows tried, the best results were obtained using a simple Gaussian window; i.e., instead of Eq. 11 we evaluate

$$G(z) = \frac{1}{2\pi} \int_{-\infty}^{\infty} \exp\left(\frac{-\mu^2}{2\sigma^2}\right) \tilde{g}_S(\mu) e^{-i\mu z}\, d\mu. \tag{23}$$

Substituting Eq. 20 into Eq. 23 we obtain the theoretical form of the spectrum:

$$G(z) = \sum_{j=0}^{N_\lambda} C_j \exp[-(z - z_j)^2\sigma^2/2], \tag{24}$$

where

$$C_j = (2\pi)^{-1/2}\sigma A_j(\lambda_j + \beta)^{-(1+\epsilon)}. \tag{25}$$

Thus, by using a window that is not identically zero for $|\mu| \geq \mu_0$, as most windows are, we obtain a spectrum that has the unusual property of having no false side peaks at all; Eq. 24 is just a sum of $N_\lambda + 1$ Gaussians with precisely one peak per component. Furthermore, the accuracy of the spectrum should be improved since $\tilde{g}_S(\mu)$ in Eq. 23 is weighted most heavily for small μ where it is most accurate and is rapidly forced toward zero for large μ where it is dominated by amplified noise.

Because $\tilde{g}_S(\mu)$ diverges quite suddenly, it is easy for the program to locate a sufficiently sharply defined divergence point, μ_0. The program then adjusts σ so that the total contribution of the integrand in Eq. 23 from the regions $|\mu| \geq \mu_0$ is between 0.1% and 0.3% of the total $G(0)$. Once σ is set, $G(z)$ is evaluated at $N_z = 201$ equally spaced points using Filon's quadrature formula (29) in Eq. 23.

The window function in Eq. 23 with a standard deviation σ produces spectral peaks in Eq. 24 with standard deviation $1/\sigma$. Thus as the accuracy and smoothness of the data increases and $\tilde{g}_S(\mu)$ remains well behaved for larger μ, a broader window with larger σ can be used, and sharper spectral peaks are obtained. In the limit $\sigma \to \infty$, Eq. 24 becomes a sum of delta functions.

Amplitude Equalization Parameter ϵ

A third difficulty with the method of Gardner et al. can be seen in Eq. 22 or 25. For $\beta = \epsilon = 0$, the amplitudes of the spectral peaks are proportional to A_j/λ_j instead of A_j. Thus components with large λ tend to get lost in the spectrum, and a base-line component with $\lambda = 0$ causes the whole solution to diverge. In our case with $\beta > 0$, we can choose an ϵ in the range $-1 < \epsilon < 0$ to reduce the effect as much as desired. However, the program constrains ϵ so that it does not approach -1 too closely and cause the first few data points to contribute too heavily to the total integral in Eq. 19.

Analysis of Gaussian Spectra

One could attempt to make σ large enough so that the individual peaks of the components were all separated, and then simply count N_λ visually. However, the errors in the spectrum increase much more rapidly with σ than does the sharpness of the peaks. In practice, far better resolution can be obtained by using our conservative criterion to select a relatively small σ and then analyzing the broader but more accurate spectral peaks with least squares. Since σ is known, the only parameters to be determined in Eq. 24 are N_λ and $\{C_j, z_j\}$, which directly yield $\{\alpha_j, \lambda_j\}$ from Eqs. 21, 25, and 17.

The N_z values of $G(z)$, $\{G_k\}$, are fit to Eq. 24 using Box's "halving and doubling" method (30, 31) for damped nonlinear least squares, but with the following modification (P. K. Rawlings, 1974, personal communication). The linear parameters $\{C_j\}$ are considered known functions of the set $\{z_j\}$; i.e., for a given $\{z_j\}$, the $\{C_j\}$ are determined by the unique *linear* least squares fit to Eq. 24. Thus the $\{C_j\}$ are constrained to their optimum values and the dimensionality of the parameter space is halved, thereby increasing the stability and rate of convergence of the nonlinear least squares fit. After the fit has converged to a solution $\{C_j^G, z_j^G\}$, the variance-covariance matrix is calculated once assuming the $\{C_j\}$ are also independent in order to obtain the usual (20) correlation coefficients and error estimates for $\{C_j^G, z_j^G\}$. The program also calculates the corresponding $\{\alpha_j^G, \lambda_j^G\}$, the theoretical values $\{G_k^G\}$ (obtained by substituting the solution into Eq. 24), and the standard deviation of the fit σ_{GG}:

$$\sigma_{GG}^2 = \sum_{k=1}^{N_z} (G_k - G_k^G)^2/(N_z - 2N_\lambda - 1). \tag{26}$$

The program first analyzes the spectrum assuming $N_\lambda = 1$ and using the maximum spectral peak for a starting guess at z_1. This solution together with the maxima of the set $|G_k - G_k^G|$ provide starting values for analyses assuming $N_\lambda = 2$, whose solutions in turn provide starting guesses for analyses assuming $N_\lambda = 3$, and so on through $N_\lambda = 5$.

Each of the N_λ solutions is further refined by using the $\{\lambda_j^G\}$ as starting guesses for a least squares fit of the raw data to Eq. 2. In addition to unit weighting, there are options for weight-

ing the raw data proportional to $y^{-1}(t)$ or $y^{-2}(t)$. In these cases the procedure of Laiken and Printz (16) is used in which the $y(t_k)$ and the corresponding weights $\{w_k\}$ are estimated from a preliminary unweighted least squares. The final least squares solution $\{\alpha_j^y, \lambda_j^y\}$ is substituted into Eq. 2 to yield the theoretical values $\{y^y(t_k)\}$ and the standard deviation, σ_{yy}:

$$\sigma_{yy}^2 = \sum_{k=1}^{n} w_k[y(t_k) - y^y(t_k)]^2/(n - 2N_\lambda - 1). \tag{27}$$

The program chooses the N_λ with the minimum

$$\sigma_{yG}^2 = \sum_{k=1}^{n} w_k[y(t_k) - y^G(t_k)]^2/(n - 2N_\lambda - 1), \tag{28}$$

where $y^G(t_k)$ is obtained by substituting $\{\alpha_j^G, \lambda_j^G\}$ into Eq. 2. This more independent criterion, in which one calculates the standard deviation of the fit of the solution from the *spectrum* to the *raw data,* was found slightly more useful than σ_{yy} even when σ_{yy} was used with the F test (20). An analogous cross-calculation of the standard deviation of the fit of the method of moments solution to the raw data would probably be a useful criterion in the component incrementation test of Isenberg et al. (11).

However, N_λ is usually obvious without resorting to any such criteria. There is usually a rapid decrease of σ_{GG} with N_λ up through the true N_λ. When too large an N_λ is used the extra components try to eliminate themselves, usually by having two z_j approach each other or by having an $|z_j| \to \infty$. The least squares fit then does not even converge, and an error exit must be taken before an arithmetic overflow occurs. This obvious choice of N_λ occurred in all the examples given in the next section.

Additional Information Input Options

The program can take advantage of optional additional information if the experimental conditions are such that: (*a*) there can be no base-line error α_0, (*b*) all the $\{\alpha_j\}$ must be positive, or (*c*) the $\{\lambda_j\}$ must be within a certain range. In the next section, only option (*a*) is used where noted, and none of them will be discussed further here.

RESULTS

For each example, a parameter set $\{\alpha_j, \lambda_j\}$ was chosen and then three sets of simulated data were produced with pseudorandom sequences of normal deviates. Nine sequences were used in all, three different ones for each of the three examples. Except where noted, the base-line component α_0 was considered unknown. The erroneous base line was produced by simply passing it through the lowest-valued data point. In all cases, the only inputs to the program were the raw data and information on whether or not $\alpha_0 = 0$, the data was in equal intervals of t, or special weighting of the data was appropriate.

For each example, only the worst of the three results is shown in Table II or III; i.e., the one with the least accurate final solution $\{\alpha_j^y, \lambda_j^y\}$. In order to separate limitations of the method from limitations inherent to errors in the data, the final solution was compared with what we call the "ideal least squares solution" (ILSS). This is the solution obtained when a conventional least squares fit of the raw data to Eq. 2 is made

TABLE I

PARAMETERS FOR SIMULATED DATA

Ex.	α	λ	RMS, root mean square error	Data weighting	No. of equally spaced points in $\underline{t}$ range	Start of $\underline{t}$ range	End of $\underline{t}$ range	$\underline{n}$, total no. of data points	$\lambda_1 t_n$*
I	-0.00015	0	0.008 × $[y(0)y(t)]^{1/2}$	$[y(t)]^{-1}$	300	0.192	57.6	300	5.9
	0.07	0.102							
	0.09	0.250							
II	-0.214	0	0.05y(t)	$[y(t)]^{-2}$	10	0	45	40	1.6
	1.029	0.0017			30	75	945		
	1.176	0.0105							
	1.190	0.0798							
III	0.00155	0	0.005y(0)	1	600	0.006	3.6	600	3.6
	0.31	1							
	0.31	3							
	0.31	9							
	0.07	27							

* The $\{\lambda_j\}$ are always subscripted in increasing order. Thus $\lambda_1 t_n$ measures how completely the decay of the longest-lived component has been observed.

using the exact values of $\{\alpha_j, \lambda_j\}$ as starting "guesses". This should give the best possible results of any method, and any errors in the ILSS could therefore be considered inherent to the data. Thus when our N_λ and $\{\alpha_j', \lambda_j'\}$ are the same as the ILSS, we say our method was "successful." All the results given in this section are "successful" ones.

Isenberg et al. (11) have used their component incrementation test with the method of moments to determine N_λ from fluorescence decay data. They increased the error level in their simulated data and showed one example where the test failed. The parameters for this set are given in example I of Table I, except that we have introduced a base-line error α_0. Also, their simulated data was convoluted with the exciting lamp flash. To partly compensate for this, n and the t range were reduced by 25%, since that is nearly the time needed for the lamp flash to reach peak intensity. Because t_n was still so large, the original $\beta = \beta_{\min}$, and only one iteration was necessary (see Table II).

In order to determine the limiting resolving power of the method, α_2/α_1, λ_2/λ_1, and the RMS were each gradually made worse until the method failed for one or more of the three pseudorandom sequences. Table III summarizes the results of successful analyses just before the failure limit. The relatively large error estimates and close σ_{yG} values for $N_\lambda = 1$ and 2 are useful warning signs that the limiting resolving power is being approached.

TABLE II

FINAL ITERATION* IN THE ANALYSES OF THE DATA FROM TABLE I

Analysis	N_λ	Fit to spectrum		Fit to raw data (final solution)		SD of fits‡		
		α^G	λ^G	$\alpha^y \pm \sigma(\alpha^y)$§	$\lambda^y \pm \sigma(\lambda^y)$§	$100\sigma_{GG}$	$100\sigma_{yy}$	$100\sigma_{yG}$
Example I	1	0.00007	0	0.00043 ± 0.00004	0	1.008	0.0588	0.1316
Iteration 1		0.146	0.159	0.141 ± 0.001	0.140 ± 0.001			
β = 0.0035	2‖	-0.00012	0	-0.00013 ± 0.00001	0	0.045	0.0161	0.0167
σ = 1.22		0.0786	0.107	0.0736 ± 0.0023	0.104 ± 0.001			
ε = -0.77		0.0825	0.270	0.0871 ± 0.0021	0.258 ± 0.006			
Example II	1	-0.166	0	0.006 ± 0.015	0	12.432	4.15	9.38
Iteration 3		1.73	0.0034	1.87 ± 0.11	0.0046 ± 0.0003			
β = 0.0002	2	-0.208	0	-0.111 ± 0.020	0	4.083	2.12	2.63
σ = 1.08		1.22	0.0020	1.24 ± 0.08	0.0026 ± 0.0002			
ε = -0.60		1.57	0.019	1.69 ± 0.22	0.0256 ± 0.0059			
	3‖	-0.223	0	-0.23 ± 0.18	0	0.280	1.76	1.79
See Fig. 1		0.968	0.0016	0.93 ± 0.15	0.0015 ± 0.0010			
		1.34	0.0103	1.19 ± 0.22	0.0088 ± 0.0032			
		1.12	0.090	1.24 ± 0.22	0.066 ± 0.020			
Example III	1	0.0052	0	0.0310 ± 0.0013	0	1.603	2.328	4.888
Iteration 3		0.638	2.08	0.783 ± 0.006	2.33 ± 0.03			
β = 0.056	2	0.0037	0	0.0093 ± 0.0006	0	0.283	0.560	0.807
σ = 1.36		0.455	1.29	0.477 ± 0.005	1.34 ± 0.01			
ε = -0.79		0.471	6.95	0.489 ± 0.005	7.89 ± 0.13			
	3	0.0031	0	0.0039 ± 0.0011	0	0.054	0.498	0.505
		0.364	1.10	0.376 ± 0.017	1.12 ± 0.04			
		0.359	3.99	0.380 ± 0.018	4.31 ± 0.36			
		0.260	12.9	0.239 ± 0.027	15.0 ± 1.4			
	4‖	0.0030	0	0.0030 ± 0.0017	0	0.015	0.497	0.499
		0.345	1.07	0.350 ± 0.040	1.07 ± 0.07			
		0.323	3.49	0.327 ± 0.060	3.59 ± 0.85			
		0.294	10.7	0.277 ± 0.054	10.7 ± 3.6			
		0.057	54	0.052 ± 0.060	36 ± 32			

* All earlier iterations were also successful and gave the same final solutions as the last iteration.

‡ See Eqs. 26-28 for definitions of σ_{GG}, σ_{yy}, and σ_{yG}.

§ $\sigma(\alpha^y)$ and $\sigma(\lambda^y)$ are the standard error estimates (20) for least squares parameters.

‖ This is the number of components with the lowest σ_{yG} and hence is the final solution. Least squares fits with larger N_λ up through $N_\lambda = 5$ were attempted, but they failed to converge and error exits had to be taken.

TABLE III

RESULTS NEAR THE LIMITS OF THE RESOLVING POWER

	Data*			Final solution				Goodness of fit vs. N_λ‡			
Ex.	α	λ	RMS	α^y	$\sigma(\alpha^y)$	λ^y	$\sigma(\lambda^y)$	N_λ	$100\sigma_{GG}$	$100\sigma_{yy}$	$100\sigma_{yG}$
Ia	-0.00019	0	0.008 ×	-0.00014	0.00002	0		1	0.222	0.0174	0.0271
	0.07	0.100	$[y(0)y(t)]^{1/2}$	0.110	0.019	0.109	0.004	2	0.031	0.0134	0.0145
	0.09	0.150		0.051	0.018	0.174	0.019				
Ib	-0.00204	0		-0.00191	0.00010	0		1	0.111	0.104	0.111
	0.96	0.102	0.008 ×	0.976	0.006	0.1028	0.0004	2	0.070	0.102	0.106
	0.04	0.250	$[y(0)y(t)]^{1/2}$	0.024	0.004	0.46	0.22				
Ic	0.00139	0	0.08 ×	0.00164	0.00015	0		1	0.256	0.202	0.216
	0.07	0.102	$[y(0)y(t)]^{1/2}$	0.110	0.012	0.123	0.006	2	0.142	0.195	0.211
	0.09	0.250		0.050	0.011	0.43	0.14				
IIIa	0	0	0.015y(0)					1	1.442	3.32	5.04
	0.31	1		0.327	0.065	1.03	0.08	2	0.255	1.54	1.66
	0.31	3		0.32	0.12	3.2	1.3	3	0.087	1.49_0	1.50
	0.31	9		0.29	0.10	10.0	6.6	4	0.034	1.49_2	1.49
	0.07	27		0.076	0.12	37.	53.				
IIIb	0	0	0.005y(0)					1	2.035	2.550	3.649
	0.43	1		0.435	0.026	1.01	0.02	2	0.244	0.391	0.509
	-0.07	3		-0.065	0.024	2.7	1.7	4	0.024	0.358	0.358
	0.43	9		0.438	0.076	9.4	1.7				
	-0.07	27		-0.085	0.11	22.	13.				

* Except for those underlined, all data parameters are the same as in Table I.

‡ When N_λ and the corresponding σ_{GG}, σ_{yy}, and σ_{yG} values are not given, the least squares fits failed to converge and error exits had to be taken.

Because our method involves numerical integration and the method of Gardner et al. requires a very wide t range, it was important to test our method using a small number of data points over a restricted t range. Example II in Table I is the one used by Laiken and Printz (16) to simulate hydrogen-exchange data, except that we have introduced a base-line error. The shortest-lived component goes through about three half-lives in the first six data points, and the optimum value of $\lambda_1 t_n$ seems to be at least four instead of 1.6. In Fig. 1 the plots of the spectrum, which are output options, graphically show the inadequacies of the data, with worse visual resolution than one might expect considering the separation of the $\{\lambda_j\}$.

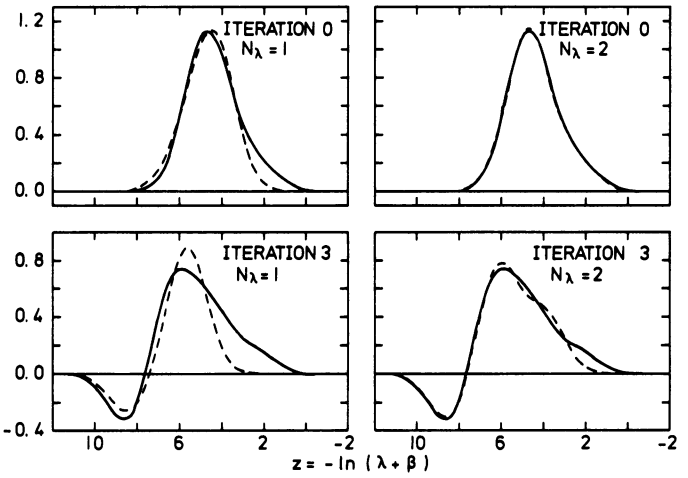

FIGURE 1 Iterative improvement of the resolution in a three-component curve, example II. The solid curves show the spectrum, $G(z)$; the broken curves show $G^G(z)$, the best least squares fit to the spectrum assuming N_λ components plus an unknown "base line" with $\lambda = 0$. In iteration 0 (the initial solution) and iteration 3 (the final solution), the $N_\lambda = 3$ fit agreed with the spectrum to within the line thickness in the drawings, and the $N_\lambda = 4$ and $N_\lambda = 5$ fits failed to converge and error exits had to be taken. The large negative baseline is clearly visible in iteration 3. In iteration 0, $\beta = 0.0034$, $\sigma = 1.05$, and $\epsilon = -0.48$; see Tables I and II for other parameter values.

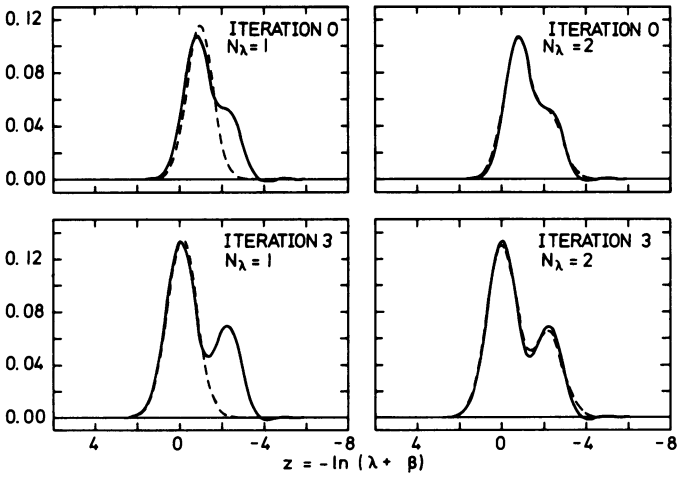

FIGURE 2 Iterative improvement of the resolution in a four-component curve, example IIIb. The solid curves show the spectrum, $G(z)$; the broken curves show $G^G(z)$, the best least squares fit to the spectrum assuming N_λ components. In iterations 0 and 3, the $N_\lambda = 3$ and $N_\lambda = 5$ fits failed to converge. The $N_\lambda = 4$ fit failed to converge in iteration 0, but in iteration 3 (the final solution) it agreed with the spectrum to within the line thickness in the drawings. In iterations 0 and 3, β was 1.26 and 0.056, σ was 1.62 and 1.42, and ϵ was -0.58 and -0.79, respectively. See Table III for other parameter values.

Example III in Table I represents the type of data that might be obtained using digital data acquisition techniques for rapid chemical relaxation kinetics (18). In Table II the closeness of σ_{yG} for $N_\lambda = 3$ and 4 is a clear warning that the failure limit is close. When the RMS, the λ ratios, or the amplitude of the shortest-lived component was made more unfavorable, both the method and the ILSS soon failed.

Although the base-line error is very small, the extra degree of freedom considerably decreases the resolving power. When it was known that $\alpha_0 = 0$, the three analyses were still successful with three times as high an RMS. This is shown in example IIIa in Table III.

All the examples so far have had all the $\{\alpha_j\}$ the same sign because this is the most difficult case. For $N_\lambda = 4$, the most difficult arrangement of $\{\alpha_j\}$ is small α_2 and α_4. The α_2 tends to get lost between the larger α_1 and α_3, and the shortest-lived α_4 contributes too little information to the data. However, when α_2 and α_4 are negative, they are considerably easier to resolve, as can be seen in example IIIb in Table III and Fig. 2.

DISCUSSION

The results show that the method is applicable over a wide range of conditions, and this is important if the program is to be truly automatic. It should be especially helpful where the other available methods have special difficulties; i.e., where N_λ is unknown and can be greater than two.

It is of course very convenient that only the raw data is needed as input, with no prejudgements or guesses required or even allowed. However the objectivity is even more important. There have already been two users who were convinced that there could not possibly be as many components as the N_λ determined by the program. In one case an instrumental problem was later found to be producing an extra component; in the other the extra component was reproducible and the postulated mechanism had to be rejected. Both had been using methods that, when combined with their biases, gave incorrect solutions and N_λ values, which nevertheless usually reproduced the data to their satisfaction.

There are of course many situations that make the concept of a completely unambiguous determination of N_λ meaningless; e.g., a λ_j can be orders of magnitude too large to be detected in the experimental t range, or two components could have practically the same λ. Thus one must always think in terms of resolving power and t range. The spectral plots, standard error estimates, and σ parameter provide objective indications of the accessible λ range and resolving power of the data.

When the conditions in Table III were further worsened so that the method did fail, the ILSS failed at the same stage or soon thereafter. Thus the method made nearly optimum use of the resolving power inherent to the data.

The results show that the resolving power decreases as the number of closely spaced components increases. Thus, to even see five or more components, one would need two or more interval sizes (as in example II) to cover the necessarily wide t range with

a reasonable number of data points. The method should have no special problems for $N_\lambda \geq 5$ provided adequate data can be obtained over the wide t range.

Computations were performed on the Univac 1108 at the Gesellschaft für wissenschaftliche Datenverarbeitung m.b.H., Göttingen.

Received for publication 24 February 1975 and in revised form 11 July 1975.

REFERENCES

1. SCHWARZ, G. 1968. Kinetic analysis by chemical relaxation methods. *Rev. Mod. Phys.* **40**:206.
2. SCHWARZ, G. 1972. Chemical relaxation of co-operative conformational transitions of linear biopolymers. *J. Theor. Biol.* **36**:569.
3. FUJITA, H. 1962. Mathematical Theory of Sedimentation Analysis. Academic Press, Inc. New York. 279–281.
4. PROVENCHER, S. W. 1967. Numerical solution of linear integral equations of the first kind. Calculation of molecular weight distributions from sedimentation equilibrium data. *J. Chem. Phys.* **46**:3229.
5. PROVENCHER, S. W., and W. GOBUSH. 1968. Two methods for the calculation of molecular-weight distributions from sedimentation-equilibrium data. *In* Characterization of Macromolecular Structure. National Academy of Sciences (U.S.A.) Publ. 1573. 143.
6. KOPPEL, D. E. 1972. Analysis of macromolecular polydispersity in intensity correlation spectroscopy: the method of cumulants. *J. Chem. Phys.* **57**:4814.
7. STOKES, A. R. 1948. A numerical Fourier-analysis method for the correction of widths and shapes of lines on x-ray powder photographs. *Proc. Phys. Soc. (Lond.).* **61**:382.
8. WASER, J., and V. SCHOMAKER. 1953. The Fourier inversion of diffraction data. *Rev. Mod. Phys.* **25**: 671.
9. ROLLETT, J. S., and L. A. HIGGS. 1962. Correction of spectroscopic line profiles for instrumental broadening by a Fourier analysis method. *Proc. Phys. Soc. (Lond.).* **79**:87.
10. TUNG, L. H. 1969. Correction of instrument spreading in gel-permeation chromatography. *J. Appl. Polymer Sci.* **13**:775.
11. ISENBERG, I., R. D. DYSON, and R. HANSON. 1973. Studies on the analysis of fluorescence decay data by the method of moments. *Biophys. J.* **13**:1090.
12. BRACEWELL, R. N., and J. A. ROBERTS. 1954. Aerial smoothing in radio astronomy. *Aust. J. Phys.* **7**:615.
13. EIGEN, M., and L. DEMAEYER. 1974. Theoretical basis of relaxation spectrometry. *In* Investigation of Rates and Mechanisms of Reactions Part II, 3rd edition. G. G. Hammes, editor. John Wiley & Sons, New York. 63.
14. PIZER, S. M., A. B. ASHARE, A. B. CALLAHAN, and G. L. BROWNELL. 1969. Fourier transform analysis of tracer data. *In* Concepts and Models of Biomathematics. F. Heinmets, editor. Marcel Dekker, New York. 105.
15. GARDNER, D. G., J. C. GARDNER, G. LAUSH, and W. W. MEINKE. 1959. Method for the analysis of multicomponent exponential decay curves. *J. Chem. Phys.* **31**:978.
16. LAIKEN, S. L., and M. P. PRINTZ. 1970. Kinetic class analysis of hydrogen-exchange data. *Biochemistry.* **9**:1547.
17. DYSON, R. D., and I. ISENBERG. 1971. Analysis of exponential curves by a method of moments, with special attention to sedimentation equilibrium and fluorescence decay. *Biochemistry.* **10**:3233.
18. JOHNSON, M. L., and T. M. SCHUSTER. 1974. Analysis of relaxation kinetics data by a nonlinear least squares method. *Biophys. Chem.* **2**:32.
19. ATKINS, G. L. 1971. A versatile digital computer program for non-linear regression analysis. *Biochim. Biophys. Acta.* **252**:405.
20. HAMILTON, W. C. 1964. Statistics in Physical Science. Ronald Press Company, New York.
21. LANCZOS, C. 1956. Applied Analysis. Prentice Hall, Englewood Cliffs, N. J. 272–280, 287.
22. TITCHMARSH, E. C. 1948. Introduction to the Theory of Fourier Integrals. Oxford University Press, London. 314.

23. GARDNER, D. G. 1963. Resolution of multi-component exponential decay curves using Fourier transforms. *Ann. N. Y. Acad. Sci.* **108**:195.
24. LIN, T. K., and J. E. DUTT. 1974. A new method for the analysis of sums of exponential decay curves. *Math. Biosci.* **20**:381.
25. ABRAMOWITZ, M., and I. A. STEGUN, editors. 1965. Handbook of Mathematical Functions. Dover Publications, New York. Eqs. 6.1.34 and 6.1.40.
26. ABRAMOWITZ, M., and I. A. STEGUN, editors. 1965. Handbook of Mathematical Functions. Dover Publications, New York. Eqs. 6.5.29 and 6.5.32.
27. BENDAT, J. S., and A. G. PIERSOL. 1971. Random Data: Analysis and Measurement Procedures. Wiley-Interscience, New York. 314.
28. PAPOULIS, A. 1973. Minimum-Bias windows for high-resolution spectral estimates. *Trans. IEEE Inf. Theory.* **IT-19**:9.
29. DAVIS, P. J., and P. RABINOWITZ. 1967. Numerical Integration. Blaisdell Publishing Co., Waltham, Mass. 62.
30. BOX, G. E. P. 1958. Use of statistical methods in the elucidation of basic mechanisms. *Bull. Inst. Int. Stat.* **36**:215.
31. BOX, G. E. P., and H. KANEMASU. 1972. Topics in model building, Part II. On nonlinear least squares. Technical Report 321. Department of Statistics, University of Wisconsin, Madison.